

1 Punctuated Aneuploidization of the Budding Yeast Genome

2 Lydia R. Heasley, Ruth A. Watson, Juan Lucas Argueso*

3
4
5
6 Department of Environmental and Radiological Health Sciences, Colorado State University, Fort
7 Collins-CO, USA

8
9
10 *Corresponding author:

11 Juan Lucas Argueso, PhD

12 493 MRB Building, 1618 campus delivery, Fort Collins, CO 80523-1618, USA

13 email: lucas.argueso@colostate.edu

14 Phone: 1-970-491-3681

15
16
17
18
19
20
21 Running Title: Genome-wide aneuploidy in yeast

22 Word Count: 2579 words

28 Abstract

29 Remarkably complex patterns of aneuploidy have been observed in the genomes of many
30 eukaryotic cell types, ranging from brewing yeasts to tumor cells (1, 2). Such aberrant karyotypes
31 are generally thought to take shape progressively over many generations, but evidence also
32 suggests that genomes may undergo faster modes of evolution (2, 3). Here, we used diploid
33 *Saccharomyces cerevisiae* cells to investigate the dynamics with which aneuploidies arise. We
34 found that cells selected for the loss of a single chromosome often acquired additional unselected
35 aneuploidies concomitantly. The degrees to which these genomes were altered fell along a
36 spectrum, ranging from simple events affecting just a single chromosome, to systemic events
37 involving many. The striking complexity of karyotypes arising from systemic events, combined with
38 the high frequency at which we detected them, demonstrates that cells can rapidly achieve highly
39 altered genomic configurations during temporally restricted episodes of genomic instability.

41 Introduction

42 Whole chromosome copy number alterations (CCNAs)(*e.g.*, aneuploidies) are an important source
43 of phenotypic variation and adaptive potential (2, 4, 5). CCNAs usually arise from defects in
44 chromosome segregation (6), but, because such errors occur rarely ($\sim 10^{-6}$ /cell/division)(7, 8), the
45 patterns by which cells accumulate extensive collections of CCNAs remain poorly understood (2).
46 Conventional paradigms of genome evolution posit that mutations (*e.g.*, CCNAs) are acquired
47 gradually and independently over many successive generations (9, 10). Cancer-centric models
48 have proposed that tumor cells can gain numerous mutations during punctuated and transient
49 bursts of genomic instability (3, 11-13), or that they become chronically destabilized and acquire
50 mutations at elevated rates (*i.e.*, mutator phenotype)(14, 15). Yet, because cancer genome
51 evolution is retrospectively inferred many generations after neoplastic initiation, our understanding
52 of how these mutagenic patterns contribute to the acquisition of CCNAs remains incomplete.

54 Results

55 We used the tractable budding yeast model system to determine the patterns by which CCNAs
56 arise. To recover spontaneously-arising aneuploid clones from populations of diploid cells, we
57 introduced the counter-selectable marker *CAN1* onto the right arm of chromosome V (Chr5R) in the
58 haploid strain JAY291 (16). Because the endogenous copy resides on Chr5L, the resulting strain
59 had two copies of *CAN1* on Chr5, one on each arm. We crossed this haploid to the S288c reference
60 strain to form a heterozygous diploid. To select for cells that had lost the JAY291 homolog of Chr5
61 (jChr5), we grew independent cultures for ≤ 35 generations in rich media and plated each onto

62 selective media containing canavanine (CAN) (17). When we visually inspected CAN-resistant
63 (CAN^R) colonies, we noted that while the majority had a normal smooth appearance, 1 in ~450
64 colonies displayed a distinctive rough morphology (Fig. 1A). Previously, we reported that this
65 morphological switch is precipitated by interhomolog mitotic recombination (MR) resulting in loss
66 of the wild type allele of the *ACE2* gene encoded on sChr12R and homozygosis of the mutant
67 *ace2-A7* allele on jChr12R (18). *ace2-A7* cells fail to separate after cytokinesis and consequently
68 form rough colonies (18, 19). In this previous study, rough colonies appeared on non-selective
69 media at a frequency of 1 in ~10,000 colonies and were always caused by MR events spanning
70 *ACE2* on Chr12R (12, 18). Rough colonies resulting from whole loss of Chr12 were never observed
71 (0/67 genotyped clones).

72

73 Our finding that rough colonies appeared >22-fold more frequently on CAN selection plates than in
74 non-selective conditions led us to hypothesize that a shared mutational process could have caused
75 the concomitant loss of jChr5 and loss-of-heterozygosity (LOH) on Chr12R. To investigate this, we
76 introduced a *URA3* marker onto sChr12L (Fig. 1B, i). Rough CAN^R clones resulting from MR
77 spanning *ACE2* would likely retain this *URA3* marker and grow on media lacking uracil (Ura⁺) (Fig.
78 1B, ii.), while rough clones caused by loss of the sChr12 homolog would be Ura⁻ (Fig. 1B, iii.). We
79 plated cultures to CAN media, screened CAN^R colonies to identify rough clones, and determined
80 the Ura^{+/-} phenotype of each. In contrast to the rough colonies recovered from non-selective
81 conditions (12, 18), 79% (41/52) of rough CAN^R colonies had lost sChr12 in addition to jChr5 (Fig.
82 1B). Our finding that the selected loss of jChr5 markedly shifted the mutational spectrum of LOH
83 on Chr12R to CCNA was consistent with our above prediction and indicated that clones harboring
84 one aneuploidy were enriched for the presence of additional unselected aneuploidies.

85

86 We performed whole-genome sequence (WGS) analysis to comprehensively define the genomic
87 structure of twenty rough CAN^R Ura⁻ clones (Table S3). The even distribution of heterozygous sites
88 across the genome of the S288c/JAY291 hybrid enabled us to detect CCNAs of each homolog and
89 changes in overall ploidy. Remarkably, the majority (65%) of the sequenced clones harbored
90 unselected CCNAs of chromosomes other than jChr5 and sChr12 (Fig. 1C, Table S3). Some clones
91 had lost numerous chromosomes (LRH279) while others displayed systemic gains (LRH266 and
92 LRH280)(Fig. 1D). Intriguingly, one clone (LRH271) had acquired CCNAs of every chromosome
93 such that both copies of one homolog had been retained while both copies of the other homolog
94 had been lost, a state known as uniparental disomy (UPD)(20). As a result of this UPD-type CCNA,

95 this clone had cumulatively gained and lost 32 homologs and was fully homozygous for either
96 parental haplotype on all chromosomes except Chr1, Chr3, and Chr9, which were tetrasomies (Fig.
97 1D). The acquisition of such numerous genomic alterations over the limited growth period of ≤ 35
98 generations suggested that these clones likely acquired all CCNAs during a temporally restricted
99 episode of chromosomal instability. The homogeneity of WGS read coverage depths observed in
100 the copy number analyses of these clones supported this conclusion. All CCNAs identified within
101 each clonal population were detected at discrete copy numbers; intermediate levels were not
102 observed (data not shown). This demonstrated that CCNAs did not continuously arise during the
103 expansion of the colony, and instead indicated that the instability underlying the formation of these
104 complex genomic alterations was short-lived.

105

106 Models of gradual mutation accumulation predict that the rate at which cells independently lose two
107 chromosomes (2^L) should be the multiplicative product of the rates at which each individual
108 chromosome is lost (1^L), referred to here as the *theoretical* 2^L rate. Our initial results challenged this
109 premise of gradual acquisition and instead suggested that multiple CCNAs could be acquired non-
110 independently. To quantitatively test this gradual model, we constructed a suite of strains in which
111 jChr5 was marked with two copies of *CAN1* and each of several S288c homologs (sChr1, sChr3,
112 sChr9, sChr12) was marked on both arms with copies of *URA3* (Fig. 2A). Plating cultures of these
113 strains to media containing CAN selected for 1^L cells that had lost jChr5, and plating to media
114 containing 5-fluoroorotic acid (5-FOA) selected for 1^L cells that had lost the *URA3*-marked homolog
115 (21). 2^L cells that had lost both marked homologs were recovered by plating on media containing
116 both CAN and 5-FOA.

117

118 We used fluctuation analysis to determine the rates at which 1^L and 2^L clones arose in ≤ 35
119 generation-cultures (Table S8). Consistent with previous reports (7, 8), 1^L clones arose at rates of
120 10^{-7} - 10^{-6} /division (Fig. 2B, yellow bars). Consequently, the *theoretical* 2^L rates for each pair of
121 aneuploidies were exceedingly low (10^{-15} - 10^{-13} /division; Fig. 2B, black lines). We found that the
122 empirically derived 2^L rates were 600- to 3800-fold higher than these *theoretical* 2^L rates (Fig. 2B,
123 striped bars), demonstrating that 2^L clones arise far more frequently than predicted by a gradual
124 model of CCNA acquisition. These results were corroborated by similar experiments in two
125 additional strains (another heterozygous strain S288c/YJM789, and an isogenic strain
126 S288c/S288c; Fig. S1 and Table S8), indicating that the higher-than-expected incidence of 2^L
127 clones was a feature common to strains from diverse genetic backgrounds.

128

129 In haploids, single aneuploidies can impair chromosomal stability and cause elevated rates of
130 subsequent CCNA acquisition (22). We considered the possibility that the 2^L clones recovered in
131 our experiments could have resulted from a similar sequential process and tested whether cells
132 aneuploid for a single chromosome exhibited substantially elevated rates of ensuing chromosome
133 loss. If the empirically-derived 2^L rates calculated above reflected such a process, then the expected
134 rates at which secondary CCNAs should be acquired would be 1100-fold greater on average
135 (1.2×10^{-4} - 1.9×10^{-3} /division, Fig. 2C, black lines) than the empirically-derived rates of a primary
136 CCNA (Fig. 2B, yellow bars). However, we found that 1^L clones (monosomic for sChr1, sChr3, jChr5,
137 or sChr9) lost a second chromosome (jChr5, sChr3, or sChr9) at rates only 2- to 12-fold greater
138 than the euploid parent and far lower than would be expected if 2^L clones arose through a process
139 of accelerated sequential accumulation (Table S8). Thus, this effect alone cannot explain the high
140 rates at which 2^L clones were recovered in our fluctuation analysis.

141

142 We performed WGS analysis of 146 1^L and 2^L isolates, as well as fifteen control clones isolated
143 from non-selective conditions. We detected no structural abnormalities in the genomes the control
144 clones. By contrast, and in agreement with our earlier results (Fig. 1), we again observed a
145 remarkable number of 1^L and 2^L clones containing additional unselected CCNAs (1^L : 39.0%; 2^L :
146 47.9%)(Fig. 3A). Of these unselected CCNAs, each of the sixteen *S. cerevisiae* chromosomes was
147 affected at similar frequencies and we found no evidence that specific CCNAs co-occurred with any
148 particular selected aneuploidy (Fig. 3B). This indicates that unselected CCNAs did not arise
149 subsequently as compensatory suppressors. Additionally, while CCNAs were by far the most
150 prevalent unselected structural genomic alteration, several clones (13/146) had also acquired tracts
151 of LOH resulting from mitotic recombination (Tables S3-S5).

152

153 We classified all 146 sequenced clones by the degree to which their genomes had been altered by
154 CCNAs (Fig. 3C). Class 1 clones lost only the selected chromosome(s) and represented 58.2% of
155 the dataset (LRH180, 85/146). The remaining 41.8% of clones contained at least one unselected
156 CCNA (61/146) and were classified as follows: Class 2 clones had additionally gained a second
157 copy of the matched homolog resulting in a UPD-type CCNA (LRH183, 21/61, 34.4%); Class 3
158 clones harbored one additional CCNA (LRH209, 19/61, 31.1%); Class 4 clones harbored multiple
159 additional CCNAs (LRH225, LRH140, LRH187, LRH85, 19/61, 31.1%); and Class 5 clones
160 harbored UPD-type CCNAs of every homolog (LRH11 and LRH159, 2/61, 3.9%).

161

162 We also sequenced the genomes of 86 1^L and 2^L isolates derived from the S288c/YJM789 hybrid.
163 Surprisingly, WGS analysis revealed that the parent strain was already trisomic for Chr12 (Fig. S2,
164 Table S5). Despite the this pre-existing CCNA, empirically derived 1^L rates for sChr1, sChr3, and
165 yChr5 in this background were comparable to the euploid S288c/JAY291 and S288c/S288c strains
166 (Fig. S1, Table S8). Similar to the clones derived from the S288c/JAY291 hybrid, numerous
167 S288c/YJM789-derived clones contained unselected CCNAs (1^L , 27%; 2^L , 40%)(Table S5).
168 Together, CCNA analysis in this background corroborated our above finding that a single pre-
169 existing CCNA, even of a chromosome as large as Chr12, did not substantially perturb genomic
170 stability, nor did it alter the patterns by which derivative clones acquired unselected CCNAs.

171

172 We modeled the number of generations required to produce class 1-5 karyotypes shown in Fig. 3C
173 if each CCNA was acquired independently at the average 1^L rate of 1.5×10^{-6} /division (Fig. 3D, black
174 dashed line). Contrary to our experimental results, this model projected that class 2-5 karyotypes
175 would have required more than 35 generations to develop gradually (41-656 generations)(Fig. 3D,
176 yellow circles). Collectively, the conventional gradual model does not effectively explain the
177 remarkable genomic complexity detected in clones from the datasets above, nor does it account for
178 the frequency at which we recovered such clones. Instead, our results are best explained by a model
179 in which multiple CCNAs are acquired during a transient burst of genomic instability.

180

181 Taken together, our results demonstrate the remarkable swiftness with which CCNAs can
182 accumulate to profoundly alter the structure and heterozygosity of a diploid genome. Indeed, cells
183 can and do acquire individual CCNAs independently, indicating that gradual accumulation of CCNAs
184 occurs. But *nearly as often*, cells acquire numerous CCNAs coincidentally. This indicates that a
185 broad spectrum of complex karyotypes can arise during stochastic and short-lived episodes, not as
186 the result of gradualism or chronic genomic instability. Our results in *S. cerevisiae* are directly
187 analogous to recent studies which suggested that it is through this punctuated mode of mutagenesis
188 that cancer cells acquire numerous copy number alterations early in tumorigenesis (3, 11, 23). What
189 cellular events might contribute to this process of punctuated copy number evolution (PCNE)(23)?
190 Perturbation of many integral cellular processes including DNA damage repair (24), replication (25),
191 sister chromatid cohesion (26), spindle assembly (27), and mitotic checkpoint activity (6) are known
192 to affect the maintenance and inheritance of chromosomes, and failure of any of these pathways
193 has the potential to affect all chromosomes in a cell equally and simultaneously (6, 28, 29). For
194 instance, even a transient failure of the mitotic checkpoint enables a cell to enter anaphase with
195 incorrect chromosome-spindle attachments. Such an erroneous mitosis could produce daughter

196 cells harboring any of the aberrant karyotypic classes described in this study (Fig. 3E)(6). Our
197 experimental approach provides a promising model system with which to meticulously define the
198 causal mechanisms of PCNE as well as to assess the phenotypic consequences and adaptive
199 potential of the remarkable karyotypes that can arise from this process.

200

201 Acknowledgements

202 We are grateful to Eric Alani, Michael McMurray, Dmitry Gordenin and Tom Petes for valuable
203 comments on the manuscript. This study was supported by NIH/NIGMS awards 1K99GM13419301
204 to LRH and R35GM11978801 to JLA.

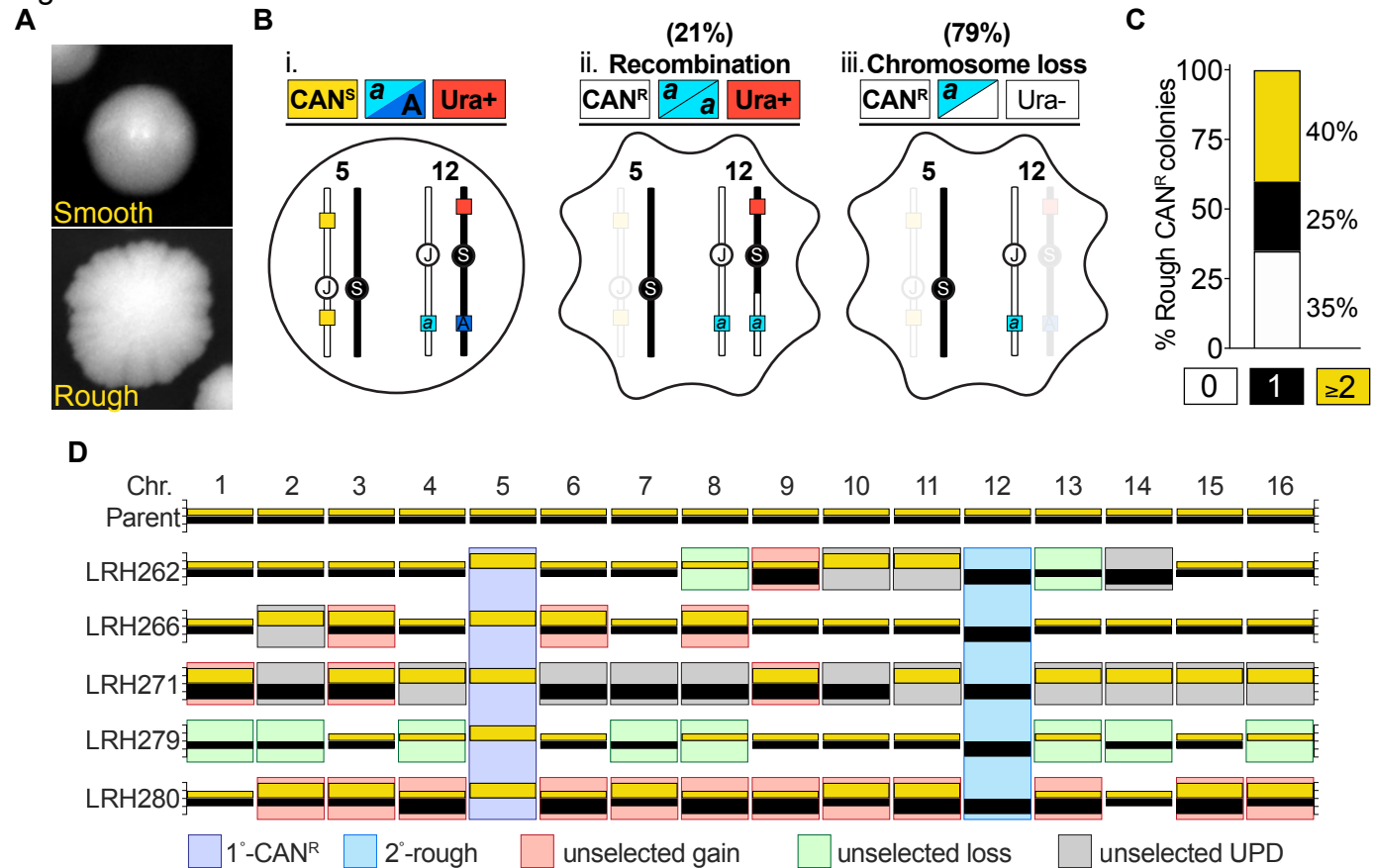
205

206 References

- 207 1. B. Gallone *et al.*, Domestication and Divergence of *Saccharomyces cerevisiae* Beer Yeasts.
208 *Cell* **166**, 1397-1410.e1316 (2016).
- 209 2. L. Sansregret, C. Swanton, The Role of Aneuploidy in Cancer Evolution. *Cold Spring Harb*
210 *Perspect Med* **7**, (2017).
- 211 3. R. Gao *et al.*, Punctuated copy number evolution and clonal stasis in triple-negative breast
212 cancer. *Nature Genetics* **48**, 1119-1130 (2016).
- 213 4. C. Gilchrist, R. Stelkens, Aneuploidy in yeast: Segregation error or adaptation mechanism?
214 *Yeast*, (2019).
- 215 5. A. M. Selmecki *et al.*, Polyploidy can drive rapid adaptation in yeast. *Nature* **519**, 349-352
216 (2015).
- 217 6. A. Musacchio, The Molecular Biology of Spindle Assembly Checkpoint Signaling Dynamics.
218 *Current biology: CB* **25**, R1002-1018 (2015).
- 219 7. H. L. Klein, Spontaneous chromosome loss in *Saccharomyces cerevisiae* is suppressed by
220 DNA damage checkpoint functions. *Genetics* **159**, 1501-1509 (2001).
- 221 8. R. Kumaran, S. Y. Yang, J. Y. Leu, Characterization of chromosome stability in diploid,
222 polyploid and hybrid yeast cells. *PLoS One* **8**, e68094 (2013).
- 223 9. C. G. A. R. Network, Comprehensive genomic characterization defines human glioblastoma
224 genes and core pathways. *Nature* **455**, 1061-1068 (2008).
- 225 10. O. Podlaha, M. Riester, S. De, F. Michor, Evolution of the cancer genome. *Trends Genet* **28**,
226 155-163 (2012).
- 227 11. M. G. Field *et al.*, Punctuated evolution of canonical genomic aberrations in uveal melanoma.
228 *Nature Communications* **9**, 116 (2018).
- 229 12. N. M. V. Sampaio *et al.*, Mitotic systemic genomic instability in yeast. *bioRxiv*, 161869 (2017).
- 230 13. N. Eldredge, S. J. Gould, in *Models of Paleobiology*, T. J. M. Schopf, Ed. (Freeman, Cooper
231 and Co., San Francisco, San Francisco., 1972), pp. 82-115.
- 232 14. L. A. Loeb, Human Cancers Express a Mutator Phenotype: Hypothesis, Origin, and
233 Consequences. *Cancer research* **76**, 2057-2059 (2016).
- 234 15. M. C. Coelho, R. M. Pinto, A. W. Murray, Heterozygous mutations cause genetic instability
235 in a yeast model of cancer evolution. *Nature* **566**, 275-278 (2019).
- 236 16. J. L. Argueso *et al.*, Genome structure of a *Saccharomyces cerevisiae* strain widely used in
237 bioethanol production. *Genome Res* **19**, 2258-2270 (2009).
- 238 17. F. W. Larimer, D. W. Ramey, W. Lijinsky, J. L. Epler, Mutagenicity of methylated N-
239 nitrosopiperidines in *Saccharomyces cerevisiae*. *Mutat Res* **57**, 155-161 (1978).

- 240 18. A. Rodrigues Prause *et al.*, A Case Study of Genomic Instability in an Industrial Strain of
241 *Saccharomyces cerevisiae*. *G3: Genes|Genomes|Genetics*, (2018).
- 242 19. B. Nelson *et al.*, RAM: a conserved signaling network that regulates Ace2p transcriptional
243 activity and polarized morphogenesis. *Molecular Biology of the Cell* **14**, 3782-3803 (2003).
- 244 20. S. L. Andersen, T. D. Petes, Reciprocal uniparental disomy in yeast. *Proc Natl Acad Sci U S*
245 *A* **109**, 9947-9952 (2012).
- 246 21. J. D. Boeke, F. LaCrute, G. R. Fink, A positive selection for mutants lacking orotidine-5'-
247 phosphate decarboxylase activity in yeast: 5-fluoro-orotic acid resistance. *Molecular &*
248 *general genetics: MGG* **197**, 345-346 (1984).
- 249 22. J. M. Sheltzer *et al.*, Aneuploidy drives genomic instability in yeast. *Science* **333**, 1026-1030
250 (2011).
- 251 23. A. K. Casasent *et al.*, Multiclonal Invasion in Breast Tumors Identified by Topographic Single
252 Cell Sequencing. *Cell* **172**, 205-217.e212 (2018).
- 253 24. R. J. Craven, P. W. Greenwell, M. Dominska, T. D. Petes, Regulation of genome stability by
254 TEL1 and MEC1, yeast homologs of the mammalian ATM and ATR genes. *Genetics* **161**,
255 493-507 (2002).
- 256 25. T. Wilhelm *et al.*, Mild replication stress causes chromosome mis-segregation via premature
257 centriole disengagement. *Nat Commun* **10**, 3585 (2019).
- 258 26. J. R. Daum *et al.*, Cohesion fatigue induces chromatid separation in cells delayed at
259 metaphase. *Current biology: CB* **21**, 1018-1024 (2011).
- 260 27. M. Mattiuzzo *et al.*, Abnormal kinetochore-generated pulling forces from expressing a N-
261 terminally modified Hec1. *PLoS One* **6**, e16307 (2011).
- 262 28. B. A. Weaver, D. W. Cleveland, Does aneuploidy cause cancer? *Curr Opin Cell Biol* **18**, 658-
263 667 (2006).
- 264 29. J. M. Nicholson, D. Cimini, How mitotic errors contribute to karyotypic diversity in cancer. *Adv*
265 *Cancer Res* **112**, 43-75 (2011).
- 266

Figure 1



267

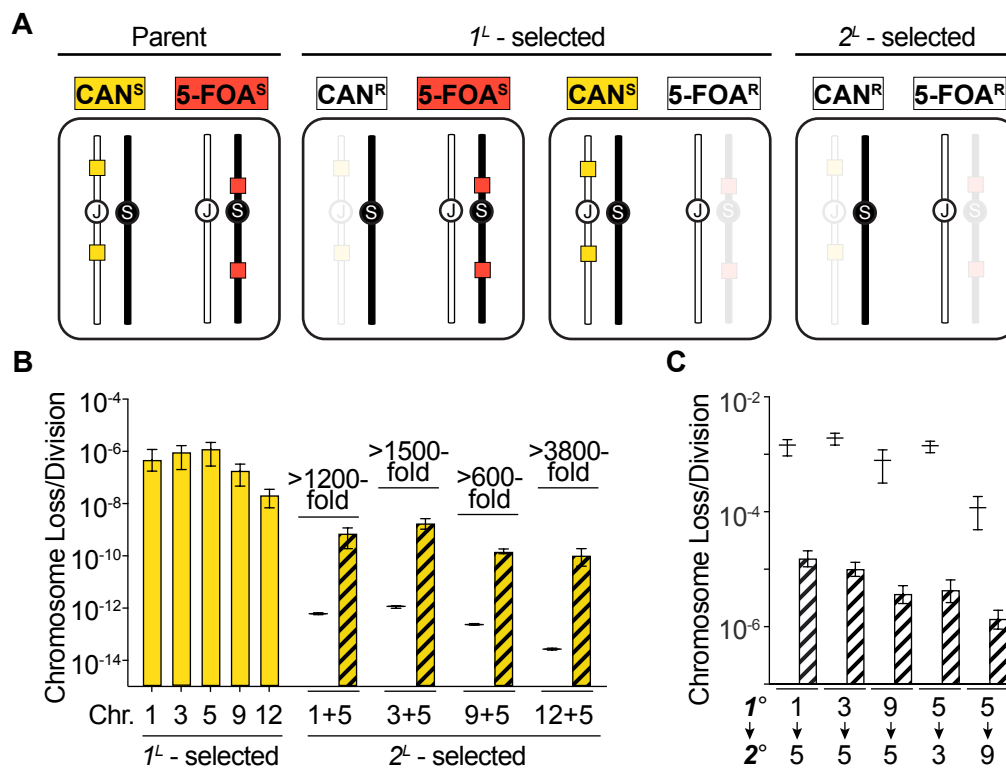
268

269 **Figure 1. Clones selected for a single CCNA are enriched for additional CCNAs.**

270 **(A)** Images of smooth and rough colonies. **(B)** A schematic illustrating the genotypic and phenotypic
 271 outcomes of selection for loss of jChr5 and homozygosity of *ace2-A7* on jChr12. jChr5-encoded
 272 *CAN1* markers, yellow boxes; jChr12-encoded *ace2-A7* mutation, light blue box; sChr12-encoded
 273 *ACE2* allele, dark blue box; sChr12-encoded *URA3* marker, red box. *i.* the parental diploid, *ii.* 21%
 274 of rough CAN^R colonies were Ura^+ and homozygous for *ace2-A7* due to MR, *iii.* 79% of rough CAN^R
 275 were Ura^- and hemizygous for *ace2-A7* due to loss of sChr12. **(C)** Percentage of rough CAN^R
 276 isolates with 0 (white), 1 (black), and ≥ 2 (yellow) unselected CCNAs. **(D)** Karyotypes of the parent
 277 strain and five rough Ura^- CAN^R isolates. For each chromosome, yellow bars denote the S288c
 278 homolog and black bars denote the JAY291 homolog. Colored boxes denote the indicated
 279 karyotypic events.

280

Figure 2



281

282

283

284 **Figure 2. Clones with multiple CCNAs arise more often than predicted by gradual models.**

285 **(A)** Schematic illustrating our quantitative CCNA selection approach. jChr5-encoded *CAN1*

286 markers, yellow boxes, S288c homolog-encoded *URA3* markers, red boxes. **(B)** Empirically derived

287 rates of each 1^L -selection (yellow) and 2^L -selection (yellow striped). Black lines denote *theoretical*

288 2^L rates. Fold change between each *theoretical* 2^L rate and empirically derived 2^L rate is noted. **(C)**

289 Empirically derived rates at which cells with a primary existing CCNA (1°) lose a second

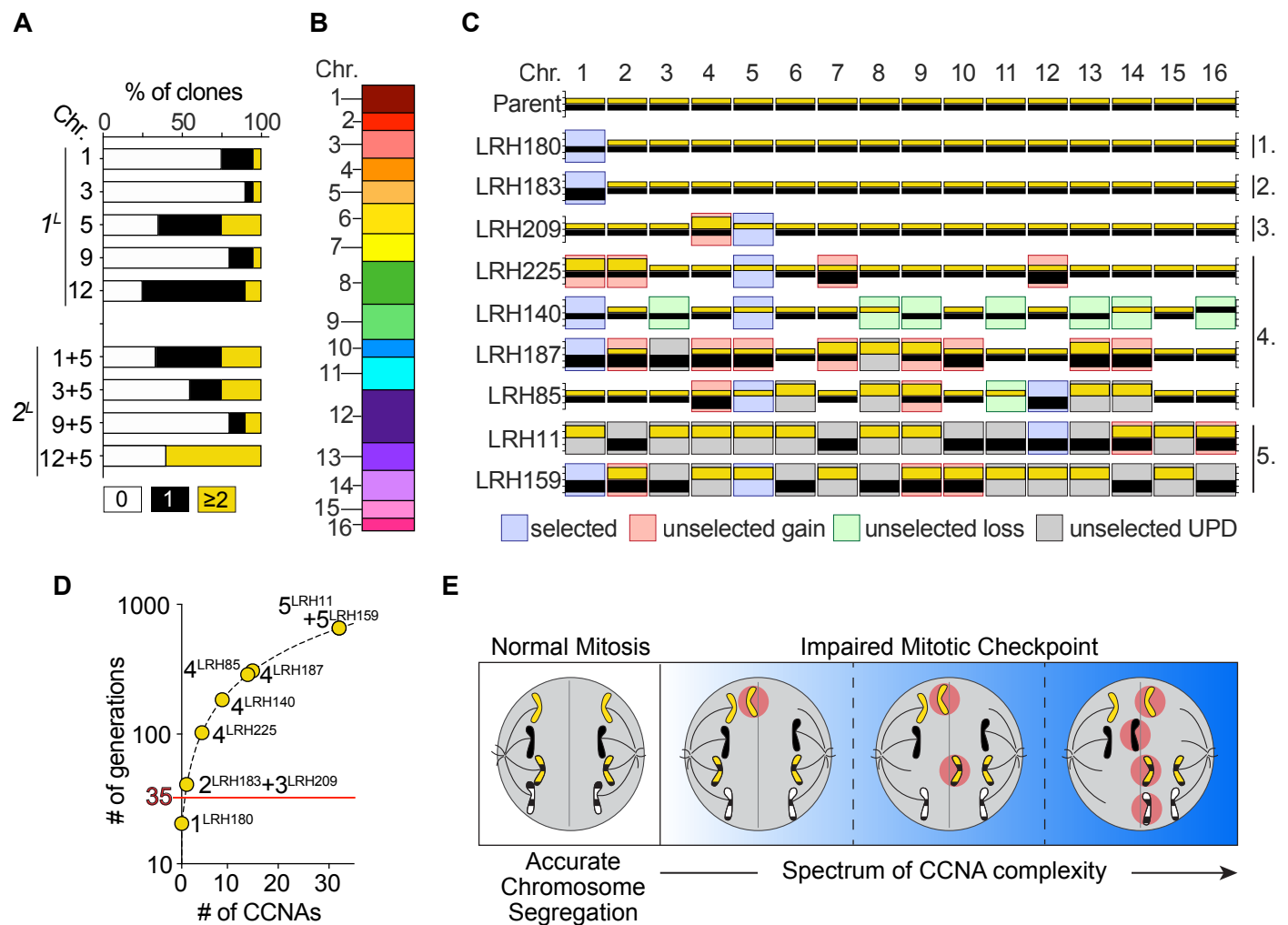
290 chromosome (2°)(striped). Black lines denote the theoretical rates at which each 2° CCNA should

291 occur if 2^L clones arise by sequential acquisition.

292

293

Figure 3



294

295 **Figure 3. 1^L and 2^L clones display a spectrum of CCNA levels.**

296 **(A)** Percentage of 1^L and 2^L isolates with 0 (white), 1 (black), and ≥2 (yellow) unselected CCNAs.

297 **(B)** Graph depicting the proportion of unselected CCNAs that affected each chromosome. **(C)**

298 Karyotypes of the parent strain and nine clones representing CCNA classes 1-5. Details as in Fig.

299 1D. **(D)** Plot depicting a model of gradual CCNA accumulation (black dashed line) and the projected

300 number of generations required to generate class 1-5 clones described in (C) (yellow circles). **(E)** A

301 model illustrating how mitosis with impaired checkpoint activity could generate cells with varying

302 numbers of CCNAs. Grey line, division plane. Red circles, mis-segregated chromosomes.

303

304 Supplementary Information Guide:

305 a) **Methods and associated references.**

306 b) **Supplementary Figure 1.** 1^L and 2^L rate analysis in two additional genetic backgrounds.

307 c) **Supplementary Figure 2.** Genomic analysis of S288c/YJM789 1^L and 2^L clones.

308 d) **Supplementary Table 1.** Yeast strains used in this study.

309 e) **Supplementary Table 2.** Plasmids used in this study.

310 f) **Supplementary Table 3.** Sequencing and copy number analysis of rough Ura- CAN^R
311 S288c/JAY291 clones.

312 g) **Supplementary Table S4.** Sequencing and copy number analysis of 1^L and 2^L S288c/JAY291
313 clones.

314 h) **Supplementary Table S5.** Sequencing and copy number analysis of 1^L and 2^L S288c/YJM789
315 clones.

316 i) **Supplementary Table S6.** Analysis of the frequency of sequenced clones possessing unselected
317 CCNAs.

318 j) **Supplementary Table S7.** Proportion of unselected CCNAs affecting each chromosome.

319 k) **Supplementary Table S8.** Rates of 1^L and 2^L chromosome loss calculated using fluctuation
320 analysis.

321

322

323 **Supplementary methods and associated references:**

324 Strain construction and culture media:

325 All *Saccharomyces cerevisiae* strains used in this study are listed in Table S1 and were derived
326 from the S288c, JAY291 (16), or YJM789 (30) backgrounds. Plasmids used for PCR-based
327 amplification of selectable markers (31-33) are listed in Table S2. Strain construction was performed
328 using standard transformation, crossing, and sporulation procedures. Specific descriptions of the
329 construction of experimental strains are outlined below. To ensure that each strain used in these
330 studies was unable to initiate meiosis and undergo a return-to-growth (RTG) process, we replaced
331 the *IME1* locus on each homolog of Chr10 with *HPHMX* selectable markers. RTG is a process in
332 which diploid yeast cells initiate meiotic programs, introduce Spo11-mediated double strand breaks
333 throughout the genome and then return to vegetative growth (34). This process can lead to
334 extensive MR-derived LOH.

335

336 Construction of *CAN1*-marked chromosomes (jChr5, yChr5, sChr5):

337 A PCR product consisting of *CAN1-KANMX* amplified from genomic DNA was integrated into the
338 *HOM3* locus on Chr5R. Resulting strains had the endogenous *CAN1* gene on Chr5L (31694-33466)
339 and the newly introduced *CAN1-KANMX* cassette on Chr5R (256375-257958).

340

341 Construction of *URA3*-marked chromosomes (sChr1, sChr3, sChr9, sChr12):

342 The *CORE3* cassette (pJA95), encodes tandem *URA3* genes from *Saccharomyces cerevisiae*
343 (*ScURA3*) and *Kluyveromyces lactis* (*KIURA3*) and a *KANMX* cassette. With the exception of Chr1
344 (see below), the full *CORE3* marker was introduced on the left arm of each S288c chromosome at
345 the coordinate listed in Table S1. Into an isogenic strain of the opposite mating type, a single
346 *KIURA3* marker was inserted into the right arm of the same chromosome at the coordinate listed in
347 Table S1. The two resulting strains were crossed, sporulated, and spores were dissected to recover
348 a haploid derivative with both the left-arm *CORE3* and right-arm *KIURA3* markers. For construction
349 of *URA3*-encoding sChr1, a *KIURA3* marker was inserted into both the left and right arms.

350

351 Construction of the *TRP1*-marked chromosome (sChr3):

352 To select for loss of sChr3 in the S288c/YJM789 hybrid, the *TRP1* gene was amplified from genomic
353 DNA and integrated into Chr3L and Chr3R at the coordinates listed in Table S1 in the intermediate
354 strains that were used to make sChr1 (above). These strains were then crossed, sporulated, and
355 spores were dissected to recover a haploid derivative encoding both *TRP1* markers and both
356 *KIURA3* markers. This strain was crossed to JAY2593 to form a heterozygous diploid in which

357 chromosomes sChr1, sChr3, and yChr5 were each marked with counter-selectable markers.
358 Although efficacy of *TRP1* counterselection was strong in the S288c/YJM789 genetic background,
359 we found it to be variable in other genetic backgrounds. For example, we discovered that this
360 selection regime was not effective in an SK1-derived background. Due to the variability of counter-
361 selection efficiency, we used only the *URA3* and *CAN1* counterselection regimes for all experiments
362 in the S288c/JAY291 background.

363

364 Media used to select CCNA clones:

365 Counterselection of *URA3* was performed by plating cells on synthetic complete media (20g/L
366 glucose, 5g/L ammonium sulfate, 1.7g/L yeast nitrogen base without amino acids, 1.4g/L complete
367 drop-out mix, 20g/L bacteriological agar) supplemented with 1g/L 5-Fluoroorotic Acid (5-FOA).
368 Counterselection of *TRP1* was performed by plating cells on synthetic complete media
369 supplemented with .75g/L 5-Fluoroanthranilic Acid (5-FAA). 5-FAA counterselection was only used
370 in plating assays and experiments in the S288c/YJM789 background. Counterselection against
371 *CAN1* was performed by plating cells on synthetic media lacking arginine (20g/L glucose, 5g/L
372 ammonium sulfate, 1.7g/L yeast nitrogen base without amino acids, 1.4g/L arginine dropout mix,
373 20g/L bacteriological agar) supplemented with 0.06g/L canavanine sulfate (CAN). Selection of 2^L
374 clones was performed by plating cells to appropriate media supplemented with 1g/L 5-FOA and
375 0.06g/L CAN, 1g/L 5-FOA and 0.75g/L 5-FAA (S288c/YJM789 only), or 0.75g/L 5-FAA and 0.06g/L
376 CAN (S288c/YJM789 only). Because most S288c chromosomes in the isogenic experiments were
377 marked with *URA3* cassettes, selection of the 2^L combinations sChr1/sChr3, sChr1/sChr9, and
378 sChr1/sChr12 was conducted by plating cells to media supplemented with 1g/L 5-FOA.

379

380 Rough Colony Screening and Analysis:

381 Diploid yeast cells of the strain JAY2775 were streaked on solid YPD media and incubated at 30°C
382 for 32 hours to allow single colonies to grow. Single colonies were each inoculated into 5 or 7mL
383 liquid YPD cultures and incubated at 30°C for another 24 hours on a rotating drum. Each culture
384 was then diluted appropriately, plated onto CAN-supplemented media, and incubated at 30°C for 4
385 days. Plates were then visually screened for the presence of rough colonies. Rough colonies were
386 isolated with a sterile toothpick and streaked onto both CAN-supplemented media (to preserve a
387 stock) and uracil-dropout media (20g/L glucose, 5g/L ammonium sulfate, 1.7g/L yeast nitrogen base
388 without amino acids, 1.4g/L uracil drop-out mix, 20g/L bacteriological agar). Plates were incubated
389 at 30°C for 24 hours. After 24 hours, each clone was assessed for its ability to grow on uracil-
390 dropout media.

391

392 Genome sequencing and analysis:

393 The genomes of 276 unselected, 1^L , and 2^L clones from either the S288c/JAY291 or S288c/YJM789
394 hybrid backgrounds were sequenced using Illumina short read whole genome sequencing. Genomic
395 DNA from each clone was isolated using the Yeastar Genomic DNA kit from Zymo Research.
396 Pooled, barcoded libraries of 96 individual genomes were generated using Seqwell plexWell-96 kits.
397 Each 96-sample library was sequenced on a single Illumina HiSeq lane. Using CLC Genomics
398 Workbench software (Qiagen), the following processing pipeline was utilized to analyze each
399 sequenced genome: Illumina reads for each genome were imported into CLC and mapped to the
400 most recent release of the yeast reference genome (R64-2-1, yeastgenome.org). Each resulting
401 read mapping file was then imported into the Nexus Copy Number software (Biodiscovery). Each
402 file was subjected to copy number and single nucleotide polymorphism (SNP) variant analysis to
403 identify the copy number of each chromosome (relative to the diploid parent) and heterozygosity at
404 >20,000 individual sites distributed across the genome. From this, we identified the following
405 structural variations: whole chromosome gains/losses, segmental duplications/deletions, and tracts
406 of loss-of-heterozygosity (LOH). LOH breakpoints identified in Nexus were confirmed manually in
407 CLC (Tables S3-S5).

408

409 Two different approaches were used to define CCNAs, and the analysis of each sequenced dataset
410 are present in Table S6: 1) the 16-chromosome pairs method; aneuploidy was defined as the
411 deviation of overall ploidy away from $2n$. Using this method, uniparental disomy was not scored as
412 an aneuploidy, despite loss of one homolog and gain of the other homolog, 2) the 32-homologs
413 method; aneuploidy was defined as the deviation in copy number of each individual homolog away
414 from $1n$. Using this method, UPDs were scored as two CCNAs. Graphs in Figs. 1C, 3A, and S2A
415 depict the results from the 32-homologs method of analysis. Results from both the 16-chromosome
416 pairs and 32-homologs analyses for each sequenced dataset are presented in Table S6.

417

418 Graphs in Figs. 3B and S2B depict the proportion of total unselected aneuploidies that affected each
419 yeast chromosome. To determine if there was a bias towards any chromosome in terms of
420 gains/losses, we used the chi square goodness of fit test to compare the distribution of observed
421 frequency of CCNA for each chromosome to the test distribution of expected null rates of 6.25% per
422 chromosome (100% divided by 16 chromosomes). From this test, we calculated a p-value of 0.109,
423 which indicated that there was no significant difference between each chromosome. Because we
424 found no evidence of biases favoring specific chromosomes, we pooled the total number of

425 unselected aneuploidies in the complete S288c/JAY291 or S288c/YJM789 dataset regardless of
426 primary selection (e.g., selection for loss of sChr1). These data are presented in Table S7.

427

428 Data Availability:

429 Sequence files for each clone in this study are available through NCBI (SRA) SUB7254181. All
430 strains and raw data presented in this study will be shared upon request.

431

432 Quantitative Chromosome Loss Assays:

433 Cultures of S288c/JAY291 diploid strains were prepared from single colonies in a manner identical
434 to that used to select for rough CAN^R clones (see above). Each culture was serially diluted and
435 plated onto YPD (non-selective), 5-FOA- and CAN-supplemented medias (1^L selection), and 5-
436 FOA+CAN-supplemented media (2^L selection). For the experiments using the S288c/YJM789
437 diploid strains, cultures were also plated onto 5-FAA-supplemented media (sChr3 1^L selection), and
438 onto 5-FOA+5-FAA- and CAN+5-FAA-supplemented media (2^L selection). Colonies on non-
439 selective and 1^L -selected plates were counted after 4 days of growth. Colonies on 2^L -selected plates
440 were counted after 6 days of growth. Colony count data were used to calculate rates and 95%
441 confidence intervals of chromosome loss using Flucalc, a MSS-MLE (Ma-Sandri-Sarkar Maximum
442 Likelihood Estimator) calculator for Luria-Delbrück fluctuation analysis (flucalc.ase.tufts.edu)(35).
443 To determine the *theoretical* rates at which 2^L clones should arise if each chromosome was lost
444 independently, the multiplicative product of both observed 1^L rates (and corresponding 95%
445 confidence intervals) was calculated as follows: theoretical rate $2^{L(ChrA+ChrB)} =$ empirically-derived
446 rate $1^{L(ChrA)}$ x empirically-derived rate $1^{L(ChrB)}$. The following rationale was used to calculate the
447 theoretical rates of sequential secondary CCNA acquisition depicted in Fig. 2C (black lines). Using
448 empirically-derived 1^L and 2^L rates (Fig. 2B and Table S8), we calculated the rate at which a
449 secondary chromosome (ChrB) would be expected to be lost following loss of a primary
450 chromosome (ChrA) if due to sequential process: theoretical sequential rate $1^{L(ChrB)} =$ empirically-
451 derived rate $2^{L(ChrA+ChrB)} /$ empirically-derived rate $1^{L(ChrA)}$. All empirically derived and *theoretical*
452 rates, 95%-confidence intervals, and number of cultures used to calculate each rate are listed in
453 Table S8.

454

455 Modeling gradual acquisition of CCNAs:

456 We modeled the generations associated with the gradual acquisition of CCNAs using the equation
457 $\#gen = \text{Log}_2((1.5 \times 10^6)^{\#A})$ in which #gen equals the number of generations, #A equals number of
458 CCNAs, and 1.5×10^6 defines a representative and constant rate of chromosome loss.

459

460

461 Supplemental References:

- 462 30. J. H. McCusker, K. V. Clemons, D. A. Stevens, R. W. Davis, Genetic characterization of
463 pathogenic *Saccharomyces cerevisiae* isolates. *Genetics* **136**, 1261-1269 (1994).
- 464 31. A. L. Goldstein, J. H. McCusker, Three new dominant drug resistance cassettes for gene
465 disruption in *Saccharomyces cerevisiae*. *Yeast (Chichester, England)* **15**, 1541-1553 (1999).
- 466 32. A. Wach, A. Brachat, R. Pöhlmann, P. Philippsen, New heterologous modules for classical
467 or PCR-based gene disruptions in *Saccharomyces cerevisiae*. *Yeast* **10**, 1793-1808 (1994).
- 468 33. H. Zhang *et al.*, Gene copy-number variation in haploid and diploid strains of the yeast
469 *Saccharomyces cerevisiae*. *Genetics* **193**, 785-801 (2013).
- 470 34. R. Laureau *et al.*, Extensive Recombination of a Yeast Diploid Hybrid through Meiotic
471 Reversion. *PLoS Genet* **12**, e1005781 (2016).
- 472 35. E. A. Radchenko, R. J. McGinty, A. Y. Aksenova, A. J. Neil, S. M. Mirkin, Quantitative
473 Analysis of the Rates for Repeat-Mediated Genome Instability in a Yeast Experimental
474 System. *Methods Mol Biol* **1672**, 421-438 (2018).

475

476

477

478

479

480

481

482

483

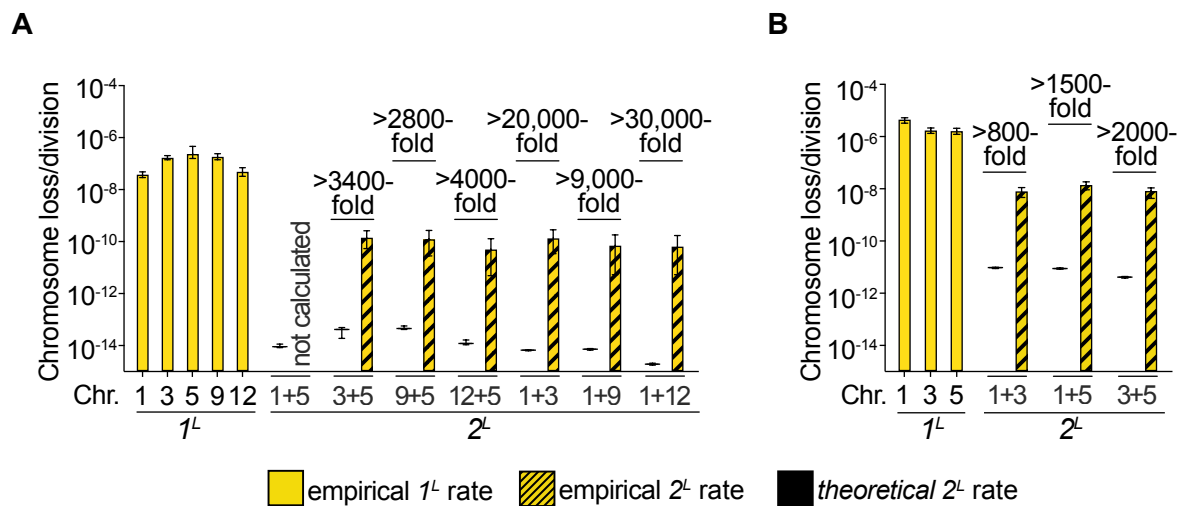
484

485

486

487

Figure S1



488

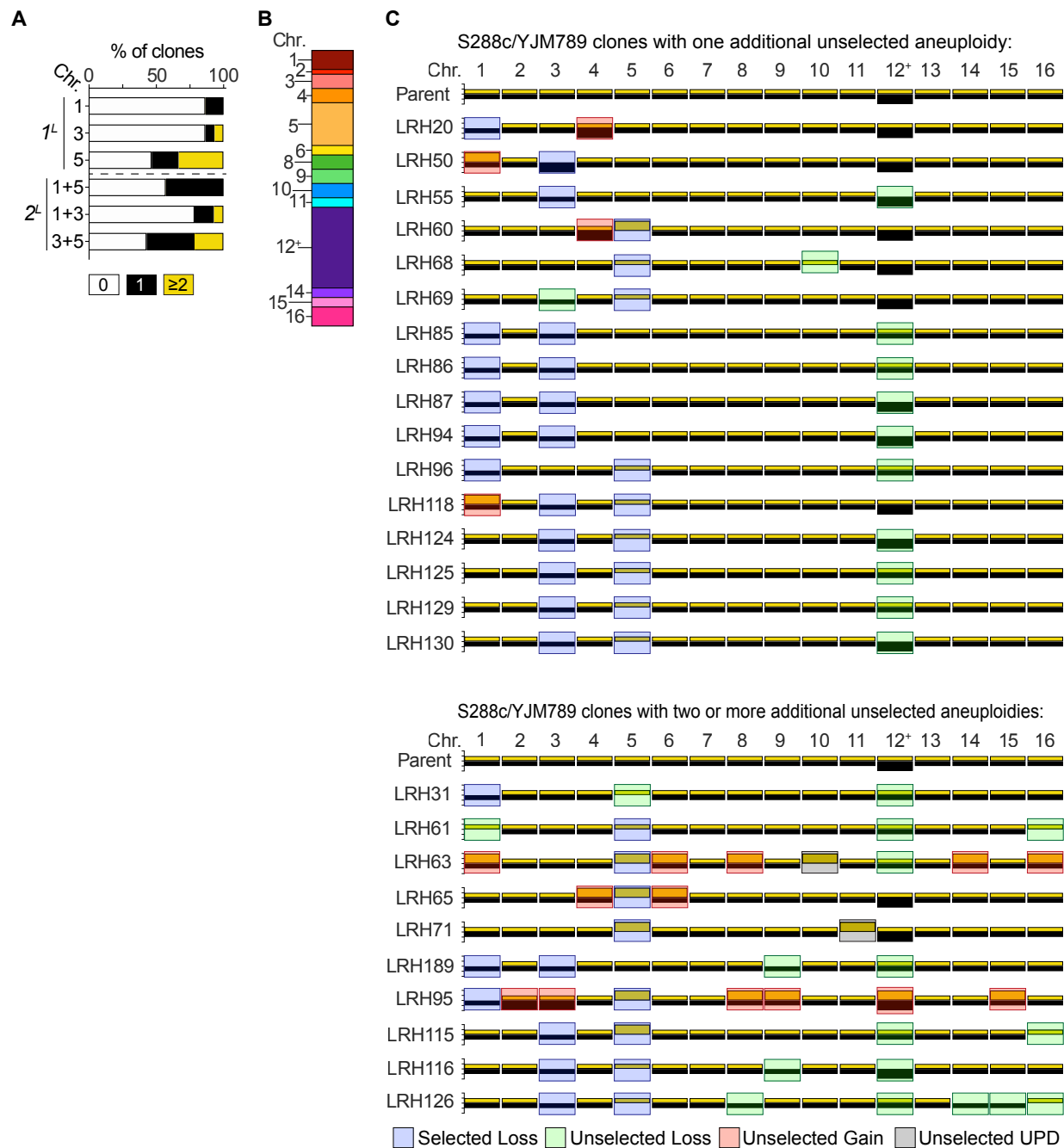
489

490 **Figure S1. 1^L and 2^L rate analysis in two diverged genetic backgrounds.** (A) Empirically derived
 491 rates of chromosome loss for each 1^L -selection (yellow) and 2^L -selection (yellow striped) in an
 492 isogenic S288c/S288c background. Black lines denote *theoretical* 2^L rate predictions. Fold change
 493 between *theoretical* 2^L rates and empirically derived 2^L rates (black lines vs. yellow striped) are
 494 noted. (B) Empirically derived rates of chromosome loss for each 1^L -selection (yellow) and 2^L -
 495 selection (yellow striped) in the hybrid S288c/YJM789 background. Black lines denote *theoretical*
 496 2^L rate predictions. Fold change between *theoretical* 2^L rates and empirically derived 2^L rates (black
 497 lines vs. yellow striped) are noted.

498

499

Figure S2



500

501

502 **Figure S2. Genomic analysis of S288c/YJM789 1^L and 2^L clones.**

503 **(A)** Percentage of 1^L and 2^L isolates with 0 (white), 1 (black), and ≥2 (yellow) unselected CCNAs.

504 **(B)** Graph depicting the proportion of unselected CCNAs affecting each chromosome. Note that

505 cells were trisomic for Chr12 (12⁺). **(C)** Karyotypes of the parent strain and all clones containing ≥1

506 unselected CCNA. For each chromosome, yellow bars denote the S288c homolog and black bars

507 denote the YJM789 homolog. yChr12 is present at two copies. Colored boxes represent denoted

508 karyotypic events.

Supplementary Table 1. Yeast Strains Used in This Study

Strain	Genotype	Background	Source	Description
S288c/JAY291 Hybrid Experiments				
JAY297	<i>MATa ura3-52 leu2Δ1 trp1Δ63</i>	S288c	Fred Winston	S288c parent
JAY298	<i>MATa ura3-52 leu2Δ1 his3Δ200</i>	S288c	Fred Winston	S288c parent
JAY1176	<i>MATa ura3</i>	JAY291	Argueso et al., 2009	JAY291 parent
JAY2736	<i>MATa trp1Δ63 leu2Δ1 can1::NATMX4 ime1::HPHMX Chr9L(94840)::CORE3 Chr9R(385386)::KIURA3</i>	S288c	LRH	sChr9
JAY2735	<i>MATa trp1Δ63 leu2Δ1 can1::NATMX4 ime1::HPHMX Chr12L(19747)::CORE3 Chr12R(402528)::KIURA3</i>	S288c	LRH	sChr12
JAY2777	<i>MATa leu2Δ1 can1::NATMX4 ime1::HPHMX Chr1L(65444)::KIURA3 Chr1R(156325)::KIURA3</i>	S288c	LRH	sChr12
JAY2778	<i>MATa can1::NATMX4 ime1::HPHMX Chr3L(91324)::CORE3 Chr3R(155596)::KIURA3</i>	S288c	LRH	sChr3
JAY2772	<i>MATa ura3 ime1::HPHMX hom3::CAN1-KANMX</i>	JAY291	LRH	jChr5
JAY2773	JAY2736 x JAY2772	JAY291 x S288c	LRH	sChr9/jChr5
JAY2775	JAY2735 x JAY2772	JAY291 x S288c	LRH	sChr12/jChr5
JAY2780	JAY2777 x JAY2772	JAY291 x S288c	LRH	sChr1/jChr5
JAY2782	JAY2778 x JAY2772	JAY291 x S288c	LRH	sChr3/jChr5
S288c/S288c Experiments				
JAY2750	<i>MATa ura3Δ52 leu2Δ1 trp1Δ63 ime1::HPHMX hom3::CAN1-KANMX/HOM3</i>	S288c	LRH	sChr5
JAY2739	<i>MATa leu2Δ1 can1::NATMX4 ime1::HPHMX Chr1L(65444)::KIURA3 Chr1R(156325)::KIURA3</i>			
JAY2828	JAY2777 x JAY2750	S288c x S288c	LRH	sChr1/sChr5
JAY2829	JAY2778 x JAY2750	S288c x S288c	LRH	sChr3/sChr5
JAY2830	JAY2736 x JAY2750	S288c x S288c	LRH	sChr9/sChr5
JAY2831	JAY2735 x JAY2750	S288c x S288c	LRH	sChr12/sChr5
JAY2832	JAY2739 x JAY2778	S288c x S288c	LRH	sChr1/sChr3
JAY2833	JAY2739 x JAY2736	S288c x S288c	LRH	sChr1/sChr9
JAY2834	JAY2739 x JAY2735	S288c x S288c	LRH	sChr1/sChr12
S288c/YJM789 Hybrid Experiments				
JAY308	<i>MATa ho::hisG, ura3, gal2</i>	YJM789	Pheobe Lee	YJM789 parent
JAY2593	<i>MATa ho::hisG, ura3, gal2 ime1::HPHMX trp1::NATMX4 hom3::CAN1-KANMX</i>	YJM789	LRH	yChr5
JAY2632	<i>MATa trp1Δ63 can1::NATMX4 ime1::HPHMX Chr1L(65444)::KIURA3 Chr1R(156325)::KIURA3 Chr3L(91324)CORE3 Chr3R(155596)KIURA3</i>	S288c	LRH	sChr1/yChr3
JAY2597	JAY2632 x JAY2593	S288c x YJM790	LRH	sChr1/sChr3/yChr5

Supplementary Table 2. Plasmids used in this study

Name	Details	Source
pJA95	<i>kiURA3-scURA3-KANMX</i>	Zhang <i>et al.</i> , 2013
pJA73	<i>pFA6a-HPHMX</i>	Goldstein <i>et al.</i> , 1999
pJA72	<i>pFA6a-NATMX</i>	Goldstein <i>et al.</i> , 1999
pJA94	<i>pFA6a-KANMX</i>	Wach <i>et al.</i> , 1994

Supplementary Table 3. Sequencing and copy number analysis of rough Ura- CANR S288c/JAY291 clones. Columns: s=S288c, j=JAY291. Selected CCNAs (jChr5 and sChr12) are highlighted in yellow. Unselected CCNAs are highlighted in red. Note: All CCNAs of sChr12 were UPD-type.

Strain	Selection	Chr1		Chr2		Chr3		Chr4		Chr5		Chr6		Chr7		Chr8		Chr9		Chr10		Chr11		Chr12		Chr13		Chr14		Chr15		Chr16		Other unselected events
		s	j	s	j	s	j	s	j	s	j	s	j	s	j	s	j	s	j	s	j	s	j	s	j	s	j	s	j	s	j	s	j	
LRH260	rough Ura- CANR	1	1	1	1	1	1	1	1	1	0	1	1	1	1	1	1	1	1	1	1	1	1	0	2	1	1	1	1	1	1	1	1	
LRH262	rough Ura- CANR	1	1	1	1	1	1	1	1	2	0	1	1	1	1	1	0	1	2	2	0	2	0	0	2	0	1	0	2	1	1	1	1	
LRH263	rough Ura- CANR	1	1	1	1	1	1	1	1	1	0	1	1	1	1	1	1	1	1	1	1	1	1	0	2	1	1	1	1	1	1	1	1	
LRH264	rough Ura- CANR	1	1	1	1	1	1	1	1	1	0	1	1	1	1	1	1	1	1	1	1	1	1	0	2	1	1	0	1	1	1	1	1	LOH JAY291 homozygous; Chr8 from 105958-TEL8R
LRH265	rough Ura- CANR	1	1	1	1	1	1	1	1	2	0	1	1	1	1	1	1	1	1	1	1	1	1	0	2	1	1	1	1	1	1	1	1	
LRH266	rough Ura- CANR	1	1	2	0	2	1	1	1	2	0	2	1	1	1	2	1	1	1	1	1	1	1	0	2	1	1	1	1	1	1	1	1	
LRH267	rough Ura- CANR	1	1	1	1	2	1	1	1	1	0	2	1	1	1	1	1	1	1	1	1	1	1	0	2	1	1	1	1	1	2	1	1	
LRH268	rough Ura- CANR	1	1	1	1	1	1	1	1	1	0	1	1	1	1	1	1	1	1	1	1	1	1	0	2	1	1	1	1	1	1	1	1	
LRH269	rough Ura- CANR	1	1	1	1	1	1	1	1	1	0	1	1	1	1	1	1	1	1	1	1	1	1	0	2	1	1	1	1	1	1	1	1	
LRH270	rough Ura- CANR	1	1	1	1	1	1	1	1	1	0	1	1	1	1	1	1	1	1	1	1	1	0	0	2	1	1	1	1	1	1	1	1	
LRH271	rough Ura- CANR	2	2	0	2	2	2	2	0	2	0	0	2	0	2	0	2	2	2	0	2	2	0	0	2	2	0	2	0	2	0	2	0	
LRH272	rough Ura- CANR	1	1	1	1	1	1	1	1	1	0	1	1	1	1	1	1	1	1	1	1	1	1	0	2	1	1	1	0	1	1	1	1	
LRH273	rough Ura- CANR	1	1	1	1	2	1	1	1	2	0	1	1	1	1	1	1	1	1	1	1	0	2	1	1	0	2	0	2	1	1	1	1	
LRH274	rough Ura- CANR	1	1	1	1	1	1	1	1	1	0	1	1	1	1	1	1	1	1	1	1	1	1	0	2	1	1	1	1	1	1	1	1	
LRH275	rough Ura- CANR	1	1	1	1	1	1	1	1	1	0	1	1	1	1	1	1	1	1	1	1	1	1	0	2	1	1	1	1	1	1	1	1	
LRH276	rough Ura- CANR	1	1	1	1	1	1	1	1	1	0	1	1	1	1	1	1	1	1	1	1	1	1	0	2	1	1	1	1	1	1	1	1	
LRH277	rough Ura- CANR	1	1	1	1	1	1	2	1	2	0	1	2	1	1	1	2	1	2	1	2	1	2	0	2	1	1	1	1	1	1	1	1	
LRH278	rough Ura- CANR	1	1	1	1	1	1	1	1	1	0	1	1	1	1	1	0	1	1	1	1	1	1	0	2	1	1	1	1	1	1	1	1	
LRH279	rough Ura- CANR	0	1	0	1	1	1	1	0	2	0	1	1	0	1	1	0	1	1	1	1	1	1	0	2	1	0	0	1	1	1	1	0	
LRH280	rough Ura- CANR	1	1	2	1	2	1	1	2	2	0	1	2	2	1	1	2	1	2	2	1	2	2	0	2	1	2	1	1	2	2	2	1	

Supplementary Table 5. Sequencing and copy number analysis of 1L and 2L S288c/YJM789 clones. Note: Diploid parent is trisomic for Chr12 (2 copies of YJM789 Chr12). Columns: s=S288c, y=YJM789. Selected CCNAs are highlighted in yellow. Unselected CCNAs are highlighted in red.

Strain	Selection	Chr1	Chr2	Chr3	Chr4	Chr5	Chr6	Chr7	Chr8	Chr9	Chr10	Chr11	Chr12	Chr13	Chr14	Chr15	Chr16	Other unselected events
		s:y	s:y	s:y	s:y	s:y	s:y	s:y	s:y	s:y	s:y	s:y	s:y	s:y	s:y	s:y	s:y	
LRH106_ys	sChr1+yChr5	0	1	1	1	1	1	1	1	1	1	1	1	2	1	1	1	1
LRH108_ys	sChr1+yChr5	0	1	1	1	1	1	1	1	1	1	1	1	2	1	1	1	1
LRH109_ys	sChr1+yChr5	0	1	1	1	1	1	1	1	1	1	1	1	2	1	1	1	1
LRH110_ys	sChr3+yChr5	0	1	1	1	1	1	1	1	1	1	1	1	2	1	1	1	1
LRH115_ys	sChr3+yChr5	1	1	1	1	0	1	1	1	1	1	1	1	1	1	1	1	1
LRH116_ys	sChr3+yChr5	1	1	1	1	0	1	1	1	1	1	1	1	0	2	1	1	1
LRH118_ys	sChr3+yChr5	2	1	1	1	0	1	1	1	1	1	1	1	1	2	1	1	1
LRH119_ys	sChr3+yChr5	1	1	1	1	0	1	1	1	1	1	1	1	1	2	1	1	1
LRH120_ys	sChr3+yChr5	1	1	1	1	0	1	1	1	1	1	1	1	1	2	1	1	1
LRH121_ys	sChr3+yChr5	1	1	1	1	0	1	1	1	1	1	1	1	1	2	1	1	1
LRH122_ys	sChr3+yChr5	1	1	1	1	0	1	1	1	1	1	1	1	1	2	1	1	1
LRH123_ys	sChr3+yChr5	1	1	1	1	0	1	1	1	1	1	1	1	1	2	1	1	1
LRH124_ys	sChr3+yChr5	1	1	1	1	0	1	1	1	1	1	1	1	0	2	1	1	1
LRH125_ys	sChr3+yChr5	1	1	1	1	0	1	1	1	1	1	1	1	1	1	1	1	1
LRH126_ys	sChr3+yChr5	1	1	1	1	0	1	1	1	1	1	1	1	1	1	0	1	1
LRH128_ys	sChr3+yChr5	1	1	1	1	0	1	1	1	1	1	1	1	1	2	1	1	1
LRH129_ys	sChr3+yChr5	1	1	1	1	0	1	1	1	1	1	1	1	1	1	1	1	1
LRH130_ys	sChr3+yChr5	1	1	1	1	0	1	1	1	1	1	1	1	0	2	1	1	1

Supplementary Table 6. Analysis of the frequency of sequenced clones possessing unselected CCNAs.			
Rough Ura- CANR clones			
	0	1	≥2
<i>16 chromosome pairs-method</i>	40.0%	25.0%	35.0%
<i>32-homologs method</i>	35.0%	25.0%	40.0%
1L and 2L S288c/JAY291 clones			
	0	1	≥2
<i>16 chromosome pairs-method</i>			
sChr1	80.00%	15.00%	5.00%
sChr3	90.00%	5.00%	5.00%
jChr5	50.00%	25.00%	25.00%
sChr9	85.00%	10.00%	5.00%
sChr12	90.00%	5.00%	5.00%
sChr1+jChr5	33.33%	50.00%	16.67%
sChr3+jChr5	60.00%	20.00%	20.00%
sChr9+jChr5	80.00%	10.00%	10.00%
sChr12+jChr5	40.00%	20.00%	40.00%
<i>32-homologs method</i>			
sChr1	75.0%	20.0%	5.0%
sChr3	90.0%	5.0%	5.0%
jChr5	35.0%	40.0%	25.0%
sChr9	80.0%	15.0%	5.0%
sChr12	25.0%	65.0%	10.0%
sChr1+jChr5	33.3%	41.7%	25.0%
sChr3+jChr5	55.0%	20.0%	25.0%
sChr9+jChr5	80.0%	10.0%	10.0%
sChr12+jChr5	40.0%	0.0%	60.0%
1L and 2L S288c/YJM789 clones			
	0	1	≥2
<i>16 chromosome pairs-method</i>			
sChr1	86.7%	13.3%	0.0%
sChr3	86.7%	13.3%	0.0%
yChr5	53.3%	26.7%	20.0%
sChr1+sChr3	64.3%	35.7%	0.0%
sChr1+yChr5	85.7%	7.1%	7.1%
sChr3+yChr5	50.0%	35.7%	14.3%
<i>32-homologs method</i>			
sChr1	86.7%	13.3%	0.0%
sChr3	86.7%	6.7%	6.7%
yChr5	46.7%	20.0%	33.3%
sChr1+sChr3	57.1%	42.9%	0.0%
sChr1+yChr5	78.6%	14.3%	7.1%
sChr3+yChr5	42.9%	35.7%	21.4%

Supplementary Table 7. Distribution of unselected CCNAs sorted by chromosome.

1L and 2L S288c/JAY291 clones																		
CCNAs per chromosome	Chr1	Chr2	Chr3	Chr4	Chr5	Chr6	Chr7	Chr8	Chr9	Chr10	Chr11	Chr12	Chr13	Chr14	Chr15	Chr16	Total	
<i>16 chromosome pairs-method</i>																		
CCNA Count	6	6	6	7	2	8	9	12	6	2	11	5	9	9	5	4	110	
% of total CCNAs	5.5	5.5	5.5	6.4	1.8	7.3	8.2	10.9	5.5	4.3	10.0	4.5	8.2	8.2	4.5	3.6		
<i>32-homologs method</i>																		
CCNA Count	11	7	11	9	9	12	11	17	14	7	13	21	11	12	7	5	177	
% of total CCNAs	6.2	4.0	6.2	5.1	5.1	6.8	6.2	9.6	7.9	4.0	7.3	11.9	6.2	6.8	4.0	2.8		
1L and 2L S288c/YJM789 clones																		
CCNAs per chromosome	Chr1	Chr2	Chr3	Chr4	Chr5	Chr6	Chr7	Chr8	Chr9	Chr10	Chr11	Chr12	Chr13	Chr14	Chr15	Chr16	Total	
<i>16 chromosome pairs-method</i>																		
CCNA Count	4	1	2	3	1	2	0	3	3	2	1	17	0	2	2	4	47	
% of total CCNAs	8.5	2.1	4.3	6.4	2.1	4.3	0.0	6.4	6.4	4.3	2.1	36.2	0.0	4.3	4.3	8.5		
<i>32-homologs method</i>																		
CCNA Count	4	1	3	3	9	2	0	3	3	3	2	17	0	2	2	4	58	
% of total CCNAs	6.9	1.7	5.2	5.2	15.5	3.4	0.0	5.2	5.2	5.2	3.4	29.3	0.0	3.4	3.4	6.9		

Supplementary Table 8. Rates of 1L and 2L chromosome loss calculated using fluctuation analysis. Light grey rows denote Theoretical 2L rate predictions calculated from empirically-derived 1L rates for each chromosome in the denoted genetic background.

S288c/JAY291 Hybrid Rates (Figure 2B)

Selection	Rate	Lower 95% difference	Upper 95% difference	Number of Cultures
Chr1	4.89E-07	2.06E-07	1.77E-07	39
Chr3	9.27E-07	2.14E-07	1.97E-07	40
Chr5	1.26E-06	3.04E-07	2.77E-07	144
Chr9	1.89E-07	5.24E-08	4.75E-08	40
Chr12	2.16E-08	8.10E-09	7.06E-09	40
Theoretical Chr1+Chr5	6.17E-13	6.24E-14	4.92E-14	
Observed Chr1+Chr5	7.44E-10	4.30E-10	5.54E-10	39
Theoretical Chr3+Chr5	1.17E-12	6.49E-14	1.75E-13	
Observed Chr3+Chr5	1.79E-09	8.72E-10	7.34E-10	40
Theoretical Chr9+Chr5	2.39E-13	1.59E-14	1.32E-14	
Observed Chr9+Chr5	1.49E-10	3.88E-11	2.67E-11	65
Theoretical Chr12+Chr5	2.73E-14	2.46E-15	1.96E-15	
Observed Chr12+Chr5	1.05E-10	8.68E-11	6.45E-11	40

S288c/S288c Isogenic Rates (Figure S1A)

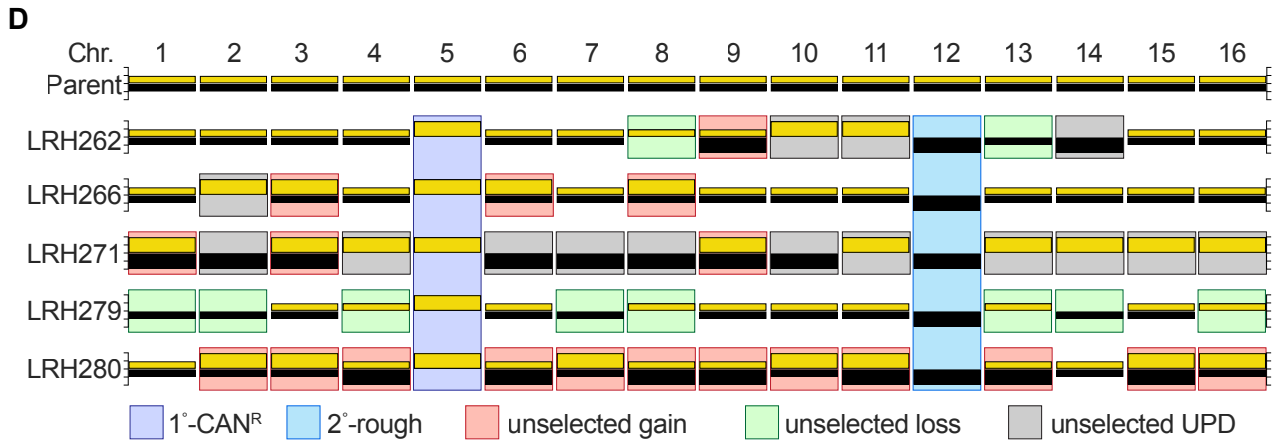
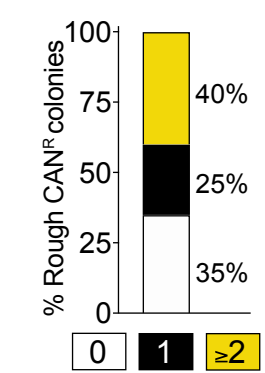
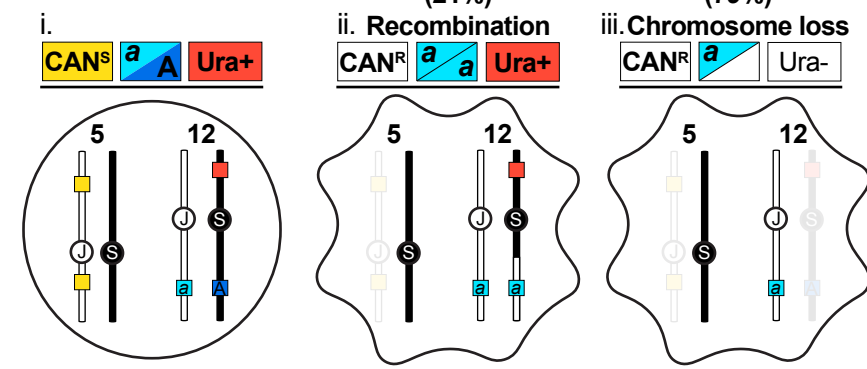
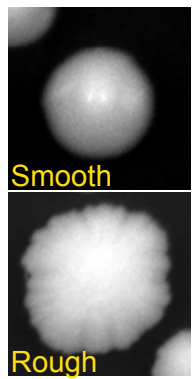
Selection	Rate	Lower 95% difference	Upper 95% difference	Number of Cultures
Chr1	3.83E-08	9.82E-09	8.97E-09	15
Chr3	1.73E-07	3.25E-08	3.04E-08	15
Chr5	2.41E-07	2.27E-07	8.26E-08	60
Chr9	1.88E-07	5.24E-08	4.75E-08	15
Chr12	5.06E-08	2.01E-08	1.75E-08	15
Theoretical Chr1+Chr5	9.24E-15	2.23E-15	7.41E-16	
Observed Chr1+Chr5	n/a	n/a	n/a	n/a
Theoretical Chr3+Chr5	4.17E-14	7.38E-15	2.26E-14	
Observed Chr3+Chr5	1.45E-10	1.21E-10	9.07E-11	30
Theoretical Chr9+Chr5	4.53E-14	1.19E-14	3.92E-15	
Observed Chr9+Chr5	1.27E-10	1.46E-10	9.90E-11	15
Theoretical Chr12+Chr5	1.22E-14	4.56E-15	1.44E-15	
Observed Chr12+Chr5	5.08E-11	7.76E-11	4.59E-11	30
Theoretical Chr1+Chr3	6.63E-15	3.19E-16	2.73E-16	
Observed Chr1+Chr3	1.37E-10	1.50E-10	1.02E-10	30
Theoretical Chr1+Chr9	7.21E-15	5.15E-16	4.26E-16	
Observed Chr1+Chr9	7.10E-11	1.14E-10	6.56E-11	15
Theoretical Chr1+Chr12	1.94E-15	1.97E-16	1.57E-16	
Observed Chr1+Chr12	6.70E-11	1.06E-10	6.16E-11	30

S288c/YJM789 Hybrid Rates (Figure S1B)

Selection	Rate	Lower 95% difference	Upper 95% difference	Number of Cultures
sChr1	4.6E-06	7.2E-07	1.3E-06	48
sChr3	1.8E-06	3.7E-07	4.5E-07	48
Chr5	1.7E-06	4.2E-07	4.4E-07	68
Theoretical Chr1+Chr3	9.6E-12	3.1E-13	6.7E-13	
Observed Chr1+Chr3	8.2E-09	3.0E-09	3.5E-09	20
Theoretical Chr1+Chr5	9.0E-12	3.6E-13	6.5E-13	
Observed Chr1+Chr5	1.4E-08	4.5E-09	5.1E-09	63
Theoretical Chr3+Chr5	4.2E-12	2.1E-13	2.8E-13	
Observed Chr3+Chr5	8.5E-09	2.5E-09	4.1E-09	76

S288c/JAY291 Sequential Loss Rates (Figure 2C)

Selection	Rate	Lower 95% difference	Upper 95% difference	Number of Cultures
Expected Chr1--> Chr5	1.45E-03	9.38E-04	1.81E-03	
Observed Chr1--> Chr5	1.57E-05	4.63E-06	5.21E-06	9
Expected Chr3--> Chr5	1.93E-03	1.45E-03	2.33E-03	
Observed Chr3--> Chr5	1.03E-05	2.68E-06	2.97E-06	10
Expected Chr9--> Chr5	7.91E-04	3.16E-04	1.20E-03	
Observed Chr9--> Chr5	3.76E-06	1.23E-06	1.40E-06	9
Expected Chr5--> Chr3	1.42E-03	1.07E-03	1.70E-03	
Observed Chr5--> Chr3	4.42E-06	1.80E-06	2.12E-06	10
Theoretical Chr5--> Chr9	1.18E-04	4.91E-05	1.85E-04	
Observed Chr5--> Chr9	1.39E-06	4.81E-07	5.53E-07	10



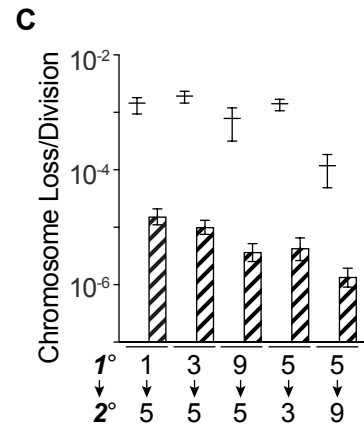
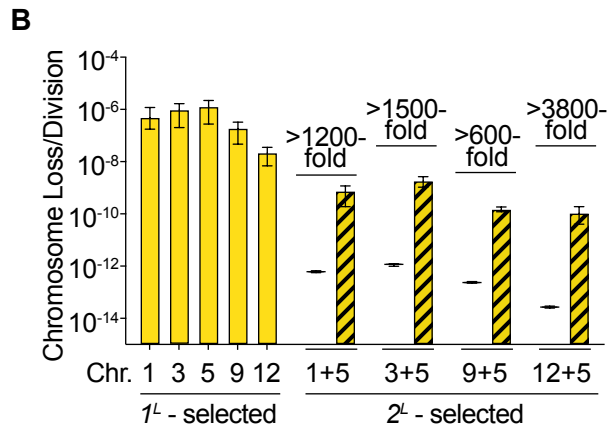
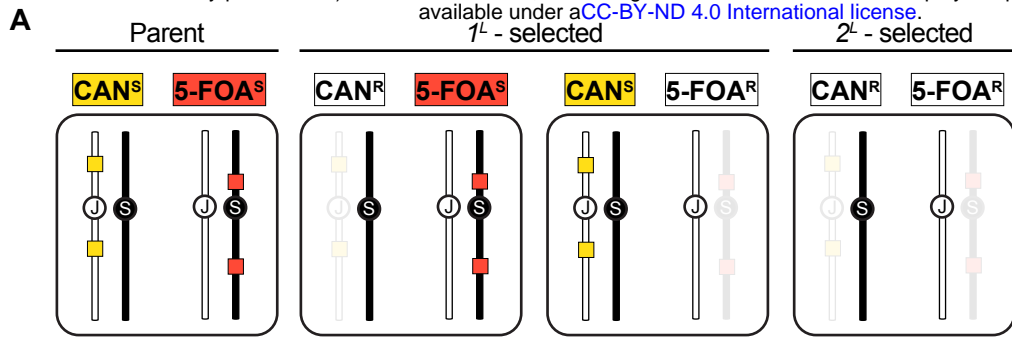
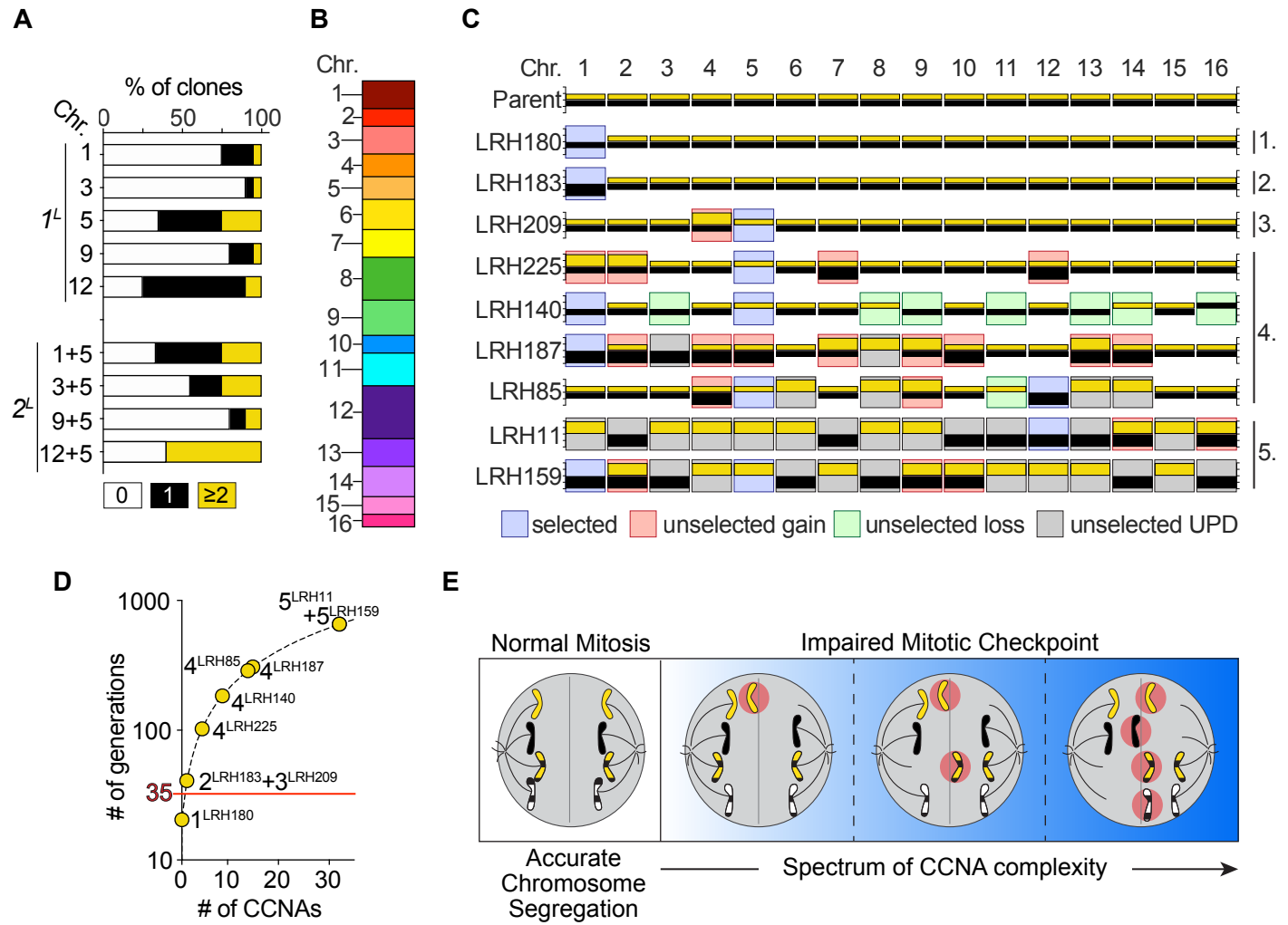
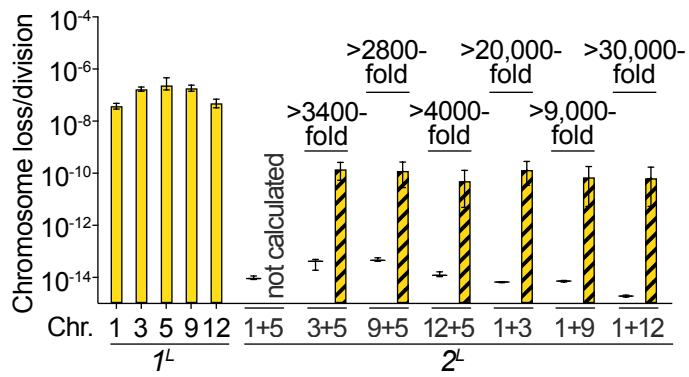


Figure 3

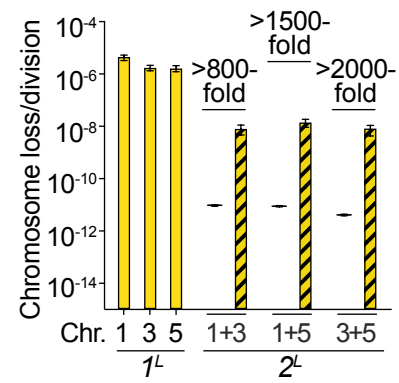


A

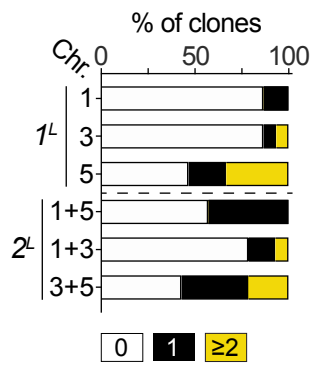


empirical 1^L rate
 empirical 2^L rate
 theoretical 2^L rate

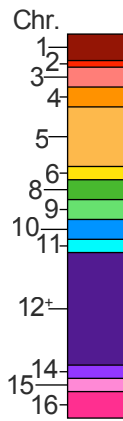
B



A



B



C

